Applied Problems of Nonlinear Oscillation and Wave Theory

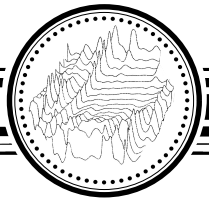

Article DOI: 10.18500/0869-6632-003198

Delocalized nonlinear vibrational modes and their effect on the properties of binary NiTi alloy

D. V. Bachurin, R. T. Murzaev✉

Institute for Metals Superplasticity Problems of the Russian Academy of Sciences, Ufa, Russia
E-mail: dvbachurin@mail.ru, ✉murzaevrt@gmail.com

Received 23.09.2025, accepted 24.10.2025, available online 24.10.2025, published 30.01.2026

Abstract. The *purpose* of this work is to investigate the behavior of stable one-component delocalized nonlinear vibrational modes in simple cubic titanium and nickel sublattices, as well as their influence on the properties of the binary NiTi alloy. *Methods.* All calculations were performed using the molecular dynamics method with many-body interatomic potentials. *Results.* Seventeen vibrational modes are shown to exhibit stable periodic oscillations. Most of them demonstrate a hard type of nonlinearity, where the frequency of atomic vibrations increases with amplitude. Stable modes are capable of accumulating energy in the range of 0.1–1.5 eV per atom in the titanium sublattice and 0.1–1.0 eV per atom in the nickel sublattice. Excitation of vibrational modes in the Ni and Ti sublattices leads to a decrease in specific heat for modes with hard type of nonlinearity and to an increase for modes with soft type of nonlinearity. The presence of modes leads to the emergence of positive compressive stresses, the magnitude of which is proportional to the atomic displacement vector. *Conclusion.* The obtained results provide new insights into the complex behavior of vibrational modes and their impact on the properties of the binary NiTi alloy.

Keywords: binary NiTi alloy, delocalized nonlinear vibrational modes, nonlinear dynamics, molecular dynamics modeling.

Acknowledgements. The work was accomplished in terms of the State Assignment of the Institute for Metals Superplasticity Problems of the Russian Academy of Sciences financed by the Ministry of Science and Higher Education of the Russian Federation, Registration No. 124022900108-3.

For citation: Bachurin DV, Murzaev RT. Delocalized nonlinear vibrational modes and their effect on the properties of binary NiTi alloy. Izvestiya VUZ. Applied Nonlinear Dynamics. 2026;34(1):98–115. DOI: 10.18500/0869-6632-003198

Introduction

Nonlinear lattices are systems in which the force of interaction between neighboring particles is nonlinearly related to their displacement from the equilibrium position. Unlike linear lattices, where the interaction follows the Hooke's law, nonlinear lattices are widely observed in physical systems such as crystals, polymers, and biological macromolecules [1, 2]. Nonlinearity can be caused by anharmonic potentials, geometric constraints, or interactions with external fields [3–5]. Such lattices play a crucial role in studying mechanical and thermal properties, energy transport, phase transitions, and the development of optical devices and waveguides [6–8].

An important consequence of nonlinearity is the emergence of localized vibrational modes, known as

discrete breathers or internal localized modes [9, 10]. These modes can exist in defect-free crystal lattices and affect their macroscopic properties [11]. High-amplitude vibrational modes have been extensively studied in nonlinear Schrodinger lattices [12, 13] and Fermi-Pasta-Ulam-Tsingou lattices [14–16], as well as in fcc lattices [17–20], bcc lattices [21–23], hcp metals [24,25], covalent crystals [26,27] and intermetallic compounds [28, 29]. To exist, discrete breathers must have a frequency outside the phonon spectrum of the crystal to avoid dissipating vibrational energy through interactions with lattice phonons.

Chechin and Sakhnenko developed the theory of bushes of nonlinear normal modes, also called delocalized nonlinear vibrational modes (DNVMs). These modes are determined based on the point group symmetry of the crystal lattice [30–32]. There is a close connection between DNVMs and discrete breathers: the latter can arise due to the modulation instability of DNVMs with frequencies beyond the phonon spectrum [33, 34]. With the development of terahertz laser technology, it has become possible to directly excite DNVMs, making them promising for photonic technologies [35, 36].

DNVMs can be conveniently classified according to their spatial dimension and the number of components. In one-dimensional DNVMs, the excited atoms form chains that are delocalized in one direction and localized in the other two. Two-dimensional DNVMs extend in two spatial directions but are localized along the third. Similarly, three-dimensional DNVMs occupy the entire volume of the crystal. One-component DNVMs have only one value of atomic displacement from their equilibrium positions, while vibrational modes with n independent parameters are referred to as n-component modes.

DNVMs affect the mechanical properties of a material, its thermal conductivity, and phase transitions. So far, most attention has been paid to one-dimensional DNVMs, for which their influence on the properties of atomic chains has been studied in detail [15, 16, 37–39]. Two-dimensional DNVMs have been widely studied in various types of crystal lattices [14,18–20,24,40,41], while the systematic study of three-dimensional DNVMs has only recently begun and has been conducted mainly in single-component materials [42–46].

In this regard, the purpose of this work is to study one-component DNVMs excited throughout the volume of the binary NiTi alloy using molecular dynamics. The choice of NiTi is based on its structure, which consists of two simple cubic lattices nested within each other, allowing for the excitation of modes in each of them. This material has promising applications in the fields of medicine and shape-memory materials [47–49].

1. Methods

1.1. Three-dimensional vibrational modes in a simple cubic lattice. Seventeen stable one-component DNVMs obtained based on the theory of bushes of nonlinear normal modes [30–32] are presented in Fig. 1 for a simple cubic lattice. These DNVMs have a delocalized character, propagating throughout the infinite crystal lattice and manifesting themselves as periodic atomic displacements. To excite these DNVMs, initial atomic displacements are specified. Fig. 1 shows two adjacent planes (001), denoted as $(001)'$ and $(002)'$, which are parallel to the (x, y) plane. The Δx and Δy displacement components in these planes are indicated by black arrows, while the Δz component is represented by red dots (for displacement towards the observer) and blue crosses (for displacement away from the observer). All nonzero atomic displacement components from their equilibrium positions in the lattice have the same amplitude A, resulting in all the modes studied in this work being one-component.

DNVMs 1, 4, 8, 12 and 23 are characterized by a single nonzero component of the displacement vector, where only $|\Delta y| = A$ or $|\Delta z| = A$, while the other components are zero. The length of the displacement vector of the atoms is equal to $D = A$. DNVMs 2, 5, 7, 9, 11, 13 and 24 have two nonzero components and a displacement vector length of $D = \sqrt{2}A$. For DNVMs 3, 6, 10, 14 and 25 , there are three nonzero components of the displacement vector, i.e., $|\Delta x| = |\Delta y| = |\Delta z| = A$, and the length of the displacement vector is $D = \sqrt{3}A$. All of these DNVMs have short wavelengths, and their wave vector lies on the boundary of the first Brillouin zone.

The seventeen stable three-dimensional DNVMs are classified according to the number of nonzero components of the atom displacements, as follows: group I includes modes with one nonzero component (DNVMs 1, 4, 8, 12, 23); group II includes modes with two nonzero components (DNVMs 2, 5, 7, 9, 11, 13, 24); and group III includes modes with three nonzero components (DNVMs 3, 6, 10, 14, 25). For

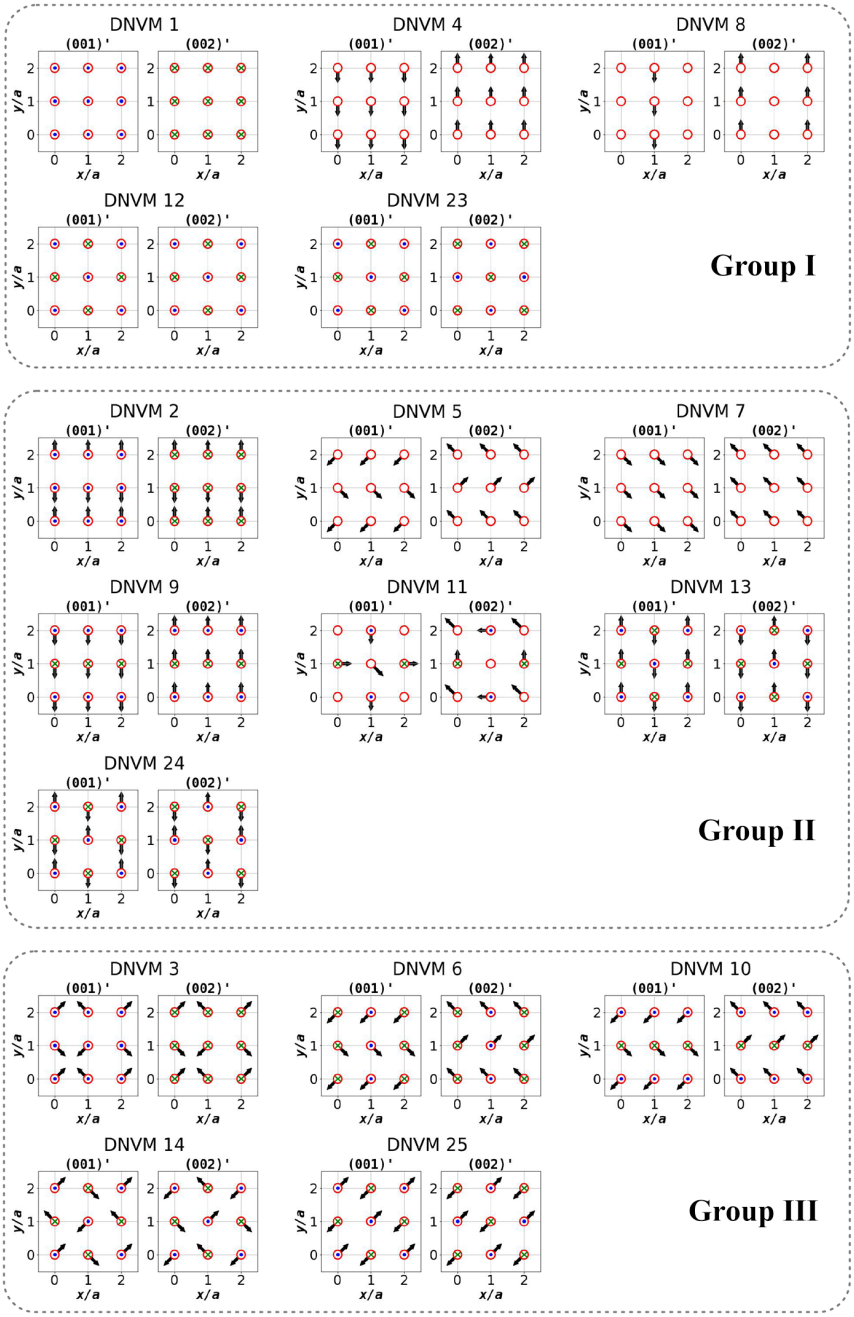

Fig. 1. Seventeen stable one-component DNVMs used to excite simple cubic sublattices of titanium or nickel atoms in the binary NiTi alloy. Atomic displacements are represented in two adjacent planes, labeled $(001)'$ and $(002)'$, parallel to the (x, y) plane. Red circles show only atoms of one cubic sublattice. The Δx and Δy components of atomic displacements along the corresponding axes from the equilibrium lattice positions are shown by black arrows. The Δz components of displacements directed toward or away from the observer are marked by blue dots and green crosses, respectively (color online)

clarity, the previously used numbering of DNVMs is retained in this work [46, 50].

1.2. The method of molecular dynamic simulation. The binary NiTi alloy has an ordered B2 structure, and the masses of the constituent elements in the alloy are close to each other: the mass of a titanium atom is 82% of the mass of a nickel atom. In the B2 structure, nickel atoms occupy the positions of a simple cubic lattice, while titanium atoms are located in the centers of the nickel sublattice, forming their own cubic sublattice.

Molecular dynamics simulations were performed using the LAMMPS software package [51, 52]. All calculations were performed using the interatomic potential developed within the framework of the modified embedded atom method (MEAM) [53]. The equilibrium lattice parameters obtained using the selected potential are $a = b = c = 2.97$ Å.

The simulation cell consists of $10 \times 10 \times 10$ translational cells of the NiTi lattice, which corresponds to 2000 atoms. Periodic boundary conditions were applied in all three orthogonal directions. The time integration step was set to 1 fs. The total simulation duration was 10000 time steps. This relatively short simulation time is due to the focus on studying the possibility of DNVMs excitation and its impact on the properties of the NiTi alloy, rather than analyzing the lifetime, which can reach several tens of picoseconds under certain conditions. The stability of the DNVMs was evaluated based on their periodic oscillations over several periods. The equations of motion were integrated using the Verlet algorithm, and the thermal fluctuations of the atoms were not taken into account to eliminate the effect of temperature. The simulation used the NVE thermodynamic ensemble, which assumes a constant number of atoms (N), volume (V), and energy (E).

The amplitudes of the initial atomic displacements used to excite the seventeen one-component vibrational modes (see Fig. 1), varied from 0.001 to 0.376 Å in steps of 0.01 Å. Initially, the atoms of one sublattice were displaced, while the atoms of the other sublattice remained stationary. The initial velocities of all atoms were set to zero.

2. Results

DNVMs 1–14 and 23–25 are stable, since they provide stable periodic oscillations over the entire volume of the simulated NiTi crystal when excited in both the nickel sublattice and the titanium sublattice, while the atoms of the adjacent sublattice remain stationary in their equilibrium positions. Note that in the unstable DNVMs 15–22, which are not considered in this work, there is a transfer of vibrational energy from one initially excited sublattice to another at all initial amplitudes.

Fig. 2, *a* shows the dependence of the displacement of the atoms Δr on the simulation time for a stable DNVM 4 excited in the nickel sublattice with initial amplitudes $A_z = 0.051$ and $A_z = 0.151$ Å. In the interval from 0 to 3 ps, periodic oscillations of nickel atoms are observed with the preservation of the initial amplitude. The titanium sublattice atoms remain unexcited, which is confirmed by the horizontal lines in Fig. 2, which overlap for two initial amplitudes. Fig. 2, *b* shows the same dependence, but in this case, the DNVM 4 is excited in the titanium sublattice. As can be clearly seen, the titanium atoms oscillate periodically, while the nickel atoms in the neighboring sublattice do not oscillate. This indicates that the stable DNVMs excited in one sublattice, even at significant initial amplitudes, does not transfer vibrational energy to the atoms in the neighboring sublattice. Similar results were obtained when other stable DNVMs 1–14 and 23–25 were excited in both sublattices.

The dependence of the oscillation frequency on the initial amplitude for the seventeen stable DNVMs in groups I, II, and III is shown in Fig. 3. In general, the different DNVMs exhibit qualitatively similar frequency characteristics. DNVMs 1 and 23 (group I), 2 and 24 (group II), and also 3, 6, 10, 14 and 25 (group III) exhibit a hard type of nonlinearity, where the frequency of atomic vibrations increases with increasing amplitude. DNVMs 5, 7, 9, 11 and 13 (group II) demonstrate a rather weak dependence of frequency on amplitude in a wide range of initial amplitudes. DNVMs 4, 8 and 12 (group I) show a soft type of nonlinearity when both sublattices are excited. DNVM 10 for the nickel sublattice and DNVMs 9, 13 and 25 for the titanium sublattice begin to exhibit soft nonlinearity at amplitudes $A > 0.3$ Å, which is due to significant deviations of the atoms from their equilibrium positions. This is due to the presence of two or three nonzero components of the displacement vector in the modes of groups II and III, which causes larger atomic displacements compared to those in group I, resulting in a soft nonlinearity. In

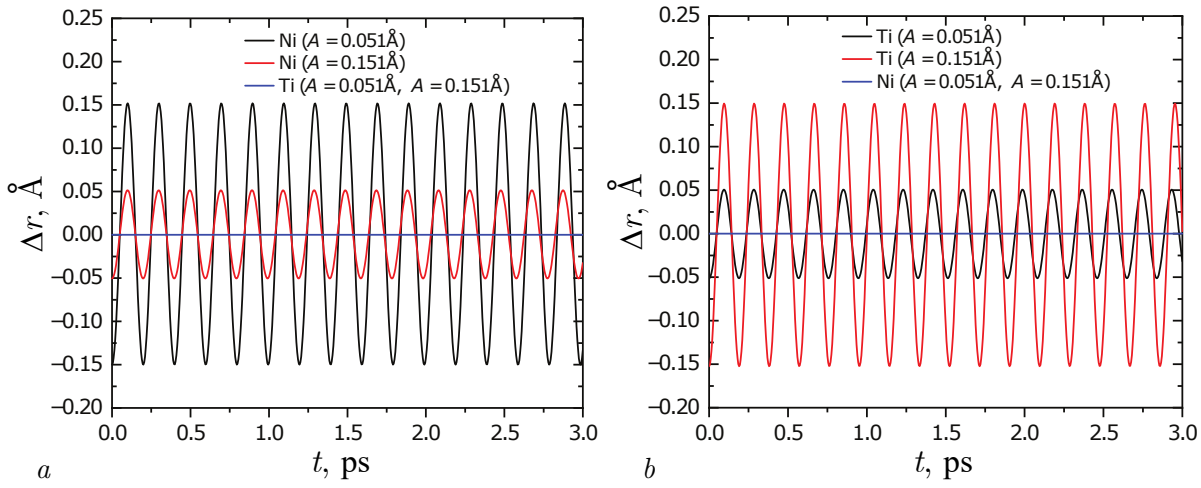

Fig. 2. The dependence of the displacement of an oscillating atom on simulation time for a stable DNVM 4 excited in nickel (a) and titanium (b) sublattices of the binary NiTi alloy. Calculations are given for two initial amplitudes $A = 0.051$ and $A = 0.151$ Å (color online)

addition, this behavior is explained by the decrease in the duration of stable periodic oscillations as the amplitude increases, which leads to the transfer of energy to neighboring atoms and the destruction of the displacement pattern characteristic of DNVMs.

As shown in Fig. 3, at small amplitudes, the frequency responses for the Ni and Ti sublattices are divided into four groups. Previous studies of one-component vibrational modes in the fcc lattice have shown that different phonon frequencies correspond to different points in the Brillouin zone [42]. The frequencies of all the studied DNVMs are in the intervals of 4.3–5.3 THz for the nickel sublattice and 5.3–6.1 THz for the titanium sublattice. When the nickel sublattice is excited, the DNVMs 23–25 have the lowest frequencies (4.3 THz), and the DNVMs 12–14 have the highest frequencies (5.3 THz).

Fig. 4 shows the dependence of the total energy (the sum of the potential and kinetic components) per atom on the initial amplitude for seventeen stable one-component DNVMs. Over the entire range of initial amplitudes, the total energy increases proportionally to the square of the displacement of the atoms from their equilibrium positions in the lattice. The absolute values of the displacement vectors for groups I, II, and III are related as $1 : \sqrt{2} : \sqrt{3}$, which determines the corresponding proportion of the total energy as $1 : 2 : 3$. Therefore, group III modes have the highest energy, followed by group II modes with lower energy, and group I modes have the lowest energy.

The analysis of the curves for the nickel sublattice revealed that the minimum and maximum total energies are 0.11 eV for DNVM 8 and 0.98 eV for DNVM 14, respectively. For the titanium sublattice, the maximum energy reaches 1.02 eV for DNVM 3, and the minimum energy reaches 0.10 eV for DNVM 8. DNVM 14 exhibits a maximum energy of 0.98 eV, followed by DNVM 3 (0.95 eV) and DNVMs 6 and 10 (0.81 eV). When DNVM 3 is excited in the titanium sublattice, its energy reaches 1.02 eV, while DNVM 14 and DNVM 25 reach 0.86 and 0.89 eV, respectively. Unlike the binary alloy Ni_3Al, where a clear separation of energy dependencies into groups [46], was previously observed, there is no such separation for NiTi. Modes from adjacent groups often have similar energy values. In addition, there can be significant differences in energy per atom within the same group, for example, between DNVM 14 and 25 (0.98 and 0.65 eV for nickel) and DNVM 3 and 10 (1.02 and 0.70 eV for titanium). These results for NiTi differ from those obtained earlier for one-component DNVM excited in the aluminum sublattice for the Ni_3Al alloy, where modes of the same group accumulate similar energy values [46].

The nonlinearity of the DNVMs was estimated by determining the ratio of the total energy of the system E_{total} to the average kinetic energy over a period of oscillation $\overline{E}_k$, namely $C = E_{\text{total}}/\overline{E}_k = 1 + \overline{E}_p/\overline{E}_k$, where $\overline{E}_p$ is the average potential energy over a period. In harmonic systems, the equality $\overline{E}_k = \overline{E}_p$ holds, which leads to $C = 2$. However, in nonlinear systems, the average kinetic energy over a period of oscillation is not equal to the average potential energy over the same period, resulting in $C \neq 2$. Thus, the deviation of the value of C from 2 serves as a characteristic of the nonlinearity of the

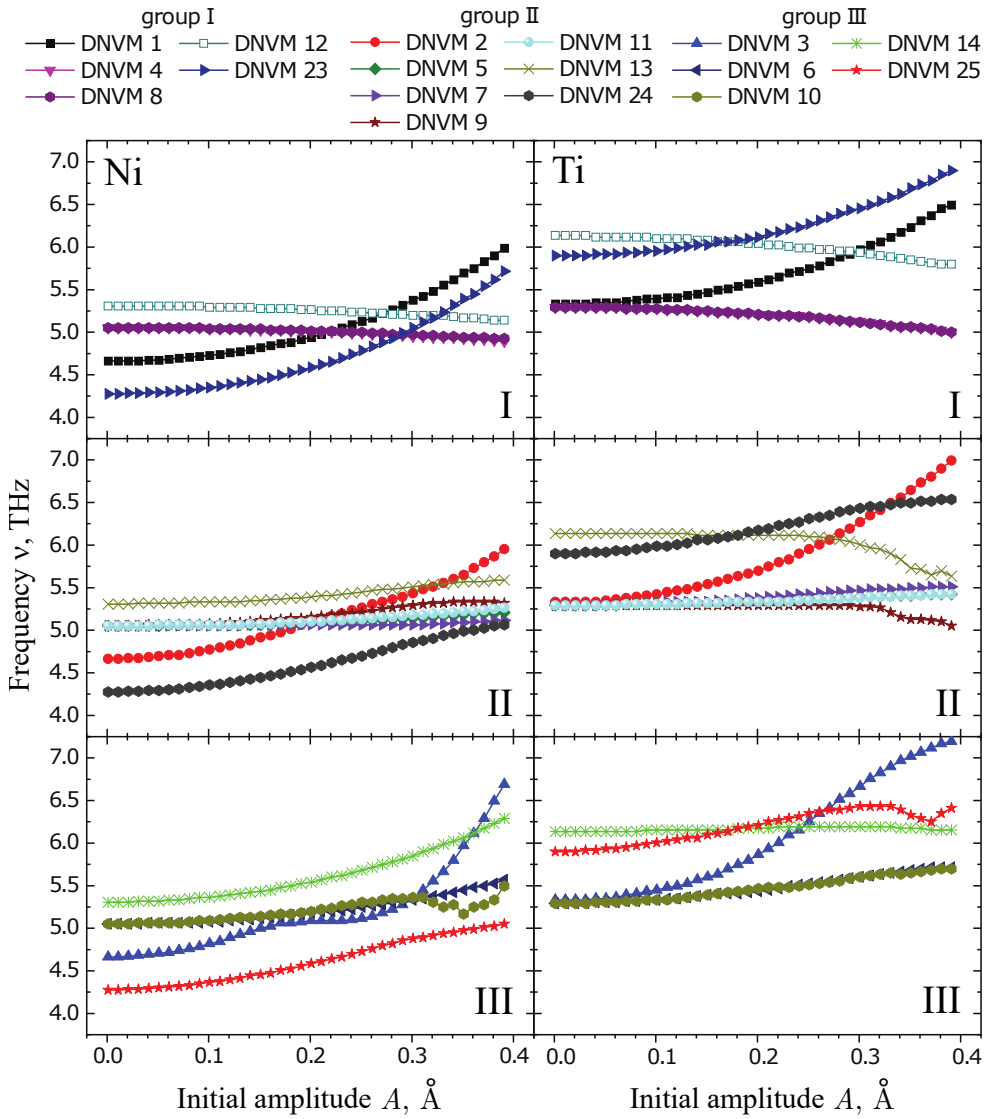

Fig. 3. Frequency characteristics of seventeen stable one-component DNVMs excited in simple cubic sublattices of nickel (left) and titanium (right) in the binary NiTi alloy. For convenience, the data are divided into three groups (I, II, III) by the number of nonzero components of the displacement vector (see text for details). The symbols "Ni" and "Ti" indicate the sublattice with excited atoms (color online)

vibrational modes and is related to the heat capacity of the crystal, as it represents the proportion of kinetic energy in the total energy of the system.

Fig. 4 shows the dependence of the ratio C on the initial amplitude for seventeen stable one-component DNVMs excited in the nickel and titanium sublattices. At small initial amplitudes $A < 0.06$ Å the nonlinearity of the DNVMs is weak for both sublattices, and the values of C change by less than 1%. However, as the amplitude increases, the DNVMs with a hard nonlinearity type show a decrease in the C ratio, while the modes with a soft nonlinearity type show an increase. In addition, as noted earlier, some DNVMs can change the type of nonlinearity as the amplitude increases, and the C ratio responds to these changes accordingly.

This behavior of the $C(A)$ dependence is explained by a simple mechanism. As the amplitude of the DNVMs oscillations with a hard type of nonlinearity increases, the frequency of the oscillations increases, which leads to an increase in the average kinetic energy $\overline{E}_k$. Since the ratio C is inversely proportional to the kinetic energy, an increase or decrease in $\overline{E}_k$ causes an increase or decrease in C, respectively.

A similar behavior of the $C(A)$ dependence is observed for other vibrational modes in various crystal lattices, including one-dimensional chains of particles [15, 39, 54], as well as two- and three-dimensional crystals [41, 44].

The application of periodic boundary conditions and the NVE (constant volume) thermodynamic ensemble during the excitation of the DNVMs leads to the generation of internal mechanical stresses in the computational cell. These stresses vary in time with a period equal to half the DNVMs oscillation period, so their time-averaged values are used for the analysis. The dependence of the hydrostatic pressure on the initial amplitude for seventeen stable DNVMs excited in the nickel and titanium sublattices is presented in Fig. 4. It is interesting to note that the hydrostatic pressure is very insignificant at low amplitudes and begins to increase significantly at initial amplitudes above $A > 0.05$ Å. As the amplitude increases further, the hydrostatic pressure on the walls of the computational cell increases, following an

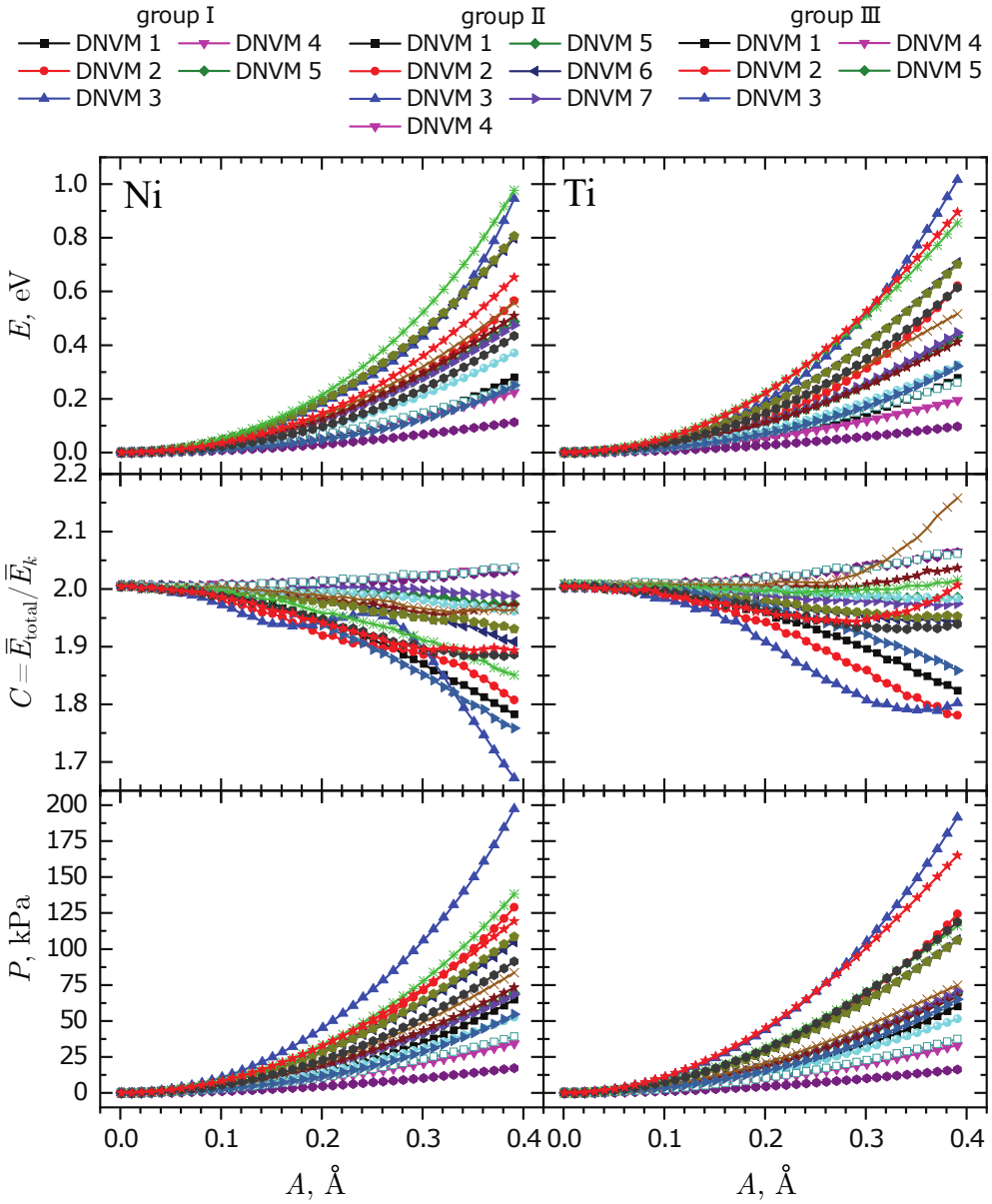

Fig. 4. Total energy per atom, the ratio C, and hydrostatic pressure as functions of the initial amplitude calculated for seventeen stable one-component DNVMs excited in the nickel and titanium sublattices in the binary NiTi alloy. The symbols "Ni" and "Ti" indicate the sublattice with excited atoms (color online)

approximately quadratic dependence. The maximum and minimum values of the hydrostatic pressure are 197 kPa for DNVM 3 and 17 kPa for DNVM 8 in the nickel sublattice, and 191 and 16 kPa respectively, in the titanium sublattice. As in the case of the total vibrational energy (see Fig. 4), there is no clear separation into mode groups. In general, there is a correlation between the vibrational energy of the modes and the generated hydrostatic pressure. The pressure values for DNVMs within the same group can vary significantly. For example, for DNVMs 3 and 6 (group III), the values in the nickel sublattice are 197 and 105 kPa, while in the titanium sublattice they are 191 and 106 kPa, respectively. Some modes from different groups, such as DNVM 2 (group II) and DNVM 25 (group III) for nickel, and DNVM 24 (group II) and DNVM 14 (group III) for titanium, generate similar values of hydrostatic pressure. In general, the one-component DNVMs excited in the nickel and titanium sublattices generate very similar values of hydrostatic pressure in the binary NiTi alloy.

It is not possible to directly compare the results obtained with those of other authors, as there are currently almost no publications dedicated to the study of one-component DNVMs in the sublattices of binary alloys. Perhaps the only exception is our previous work [55], which extensively investigated twenty-five one-component DNVMs excited in the simple cubic sublattice of aluminum throughout the binary alloy Ni_3Al. Therefore, further comparisons are approximate.

In the work [55] it was found that only sixteen DNVMs 1–4, 6, 7, 9, 12–15, 18, 20, 23–25, support stable periodic oscillations, while nine DNVMs 5, 8, 10, 11, 16, 17, 19, 21, 22 are unstable. Thus, unlike the NiTi alloy, Ni_3Al has a different set of stable and unstable vibrational modes, which is due to the differences in the symmetry of the crystal lattice affecting the dynamics of atoms for some DNVMs. It should be noted that DNVMs 1–4, 6, 7, 9, 12–14, 23–25 are stable, and DNVMs 16, 17, 19, 21, 22 are unstable in both binary alloys.

The values of the total vibrational energy accumulated by the DNVMs in Ni_3Al are comparable to those for NiTi. However, unlike in Ni_3Al, the differences in total energy within a single mode group are significantly higher in NiTi. The DNVMs excited in NiTi cause significant deviations in the C parameter, indicating a more pronounced nonlinearity and a greater contribution to the specific heat capacity of the crystal. It is important to note that the present study and the publication [55] used a computational cell of the same size, making this comparison valid. Therefore, the same DNVMs excited on structurally equivalent sublattices of different binary alloys may exhibit different amplitude-frequency characteristics and have varying effects on the properties of the crystal. At this stage of the research, it is not possible to conclude that the DNVMs studied will behave similarly in any binary alloy with a similar crystal lattice. This issue requires further investigation.

The study of DNVMs in binary alloys using molecular dynamics methods with multi-particle interatomic potentials remains a relatively narrowly specialized field, and detailed data for other alloys is extremely limited. A significant part of previous studies relied on simplified pairwise interatomic potentials, such as the Morse or β-Fermi–Pasta–Ulam–Tsingou (β-FPUT) potentials, which do not fully account for the complexity of bonds in real materials, especially in metal alloys, where multi-particle effects and angular dependencies play a key role [14, 16, 41, 43, 55–60]. This significantly limits the ability to quantitatively compare the results of these studies with the present work.

Conclusion

Using the molecular dynamics method, one-component three-dimensional DNVMs were excited in the cubic nickel and titanium sublattices of a binary NiTi alloy. These seventeen vibrational modes support stable periodic oscillations. When the modes are excited in one sublattice, their energy is localized in that sublattice and is not transferred to the other sublattice. In the investigated range of amplitudes, stable DNVMs can accumulate vibrational energy ranging from 0.11 to 0.98 eV in the nickel sublattice and from 0.10 to 1.02 eV in the titanium sublattice per atom. The amount of accumulated energy is determined by the number of nonzero components of the atomic displacement vector and is proportional to the square of the initial displacement. The excitation of DNVMs leads to a decrease in the specific heat capacity of the crystal (the ratio of total energy to kinetic energy) for modes with a hard nonlinearity, while the heat capacity increases for modes with a soft nonlinearity. The excitation of stable DNVMs in the nickel and titanium sublattices results in a hydrostatic pressure that is proportional to the length

of the atomic displacement vector. The pressure caused by DNVMs from group III is greater than the pressure caused by modes from groups I and II.

References

1. Shi JC, Zeng LW, Chen JB. Two-dimensional localized modes in saturable quintic nonlinear lattices. Nonlinear Dyn. 2023;111(14):13415–13424. DOI: 10.1007/s11071-023-08558-9.
2. Russell FM, Archilla JFR. Intrinsic localized modes in polymers and hyperconductors. Low Temp. Phys. 2022;48(12):1009–1014. DOI: 10.1063/10.0015109.
3. Abbagari S, Houwe A, Akinyemi L, Bouetou TB. Modulated wave patterns brought by higher-order dispersion and cubic-quintic nonlinearity in monoatomic chains with anharmonic potential. Wave Motion. 2023;123:103220. DOI: 10.1016/j.wavemoti.2023.103220.
4. Hall DA. Review nonlinearity in piezoelectric ceramics. Journal of Materials Science. 2001; 36(19):4575–4601. DOI: 10.1023/A:1017959111402.
5. Zhang YN, Wu JY, Jia LN, Qu Y, Yang YY, Jia BH, Moss DJ. Graphene oxide for nonlinear integrated photonics. Laser Photonics Reviews. 2023;17(3):2200512. DOI: 10.1002/lpor.202200512.
6. Sun T, Shao LH, Zhang K. Anomalous heat conduction and thermal rectification in weak nonlinear lattices. Eur. Phys. J. B. 2023;96(7):99. DOI: 10.1140/epjb/s10051-023-00568-1.
7. Ren BQ, Arkhipova AA, Zhang YQ, Kartashov YV, Wang HG, Zhuravitskii SA, Skryabin NN, Dyakonov IV, Kalinkin AA, Kulik SP, Kompanets VO, Chekalin SV, Zadkov VN. Observation of nonlinear disclination states. Light: Science and Applications. 2023;12(1):194. DOI: 10.1038/s41377-023-01235-x.
8. Kang J, Liu T, Yan M, Yang DD, Huang XJ, Wei RS, Qiu JR, Dong GP, Yang ZM, Nori F. Observation of square-root higher-order topological states in photonic waveguide arrays. Laser and Photonics Reviews. 2023;17(6):2200499. DOI: 10.1002/lpor.202200499.
9. Dolgov AS. On localization of oscillations in nonlinear crystal structure. Sov. Phys. Solid State. 1986;28:907–910.
10. Sievers AJ, Takeno S. Intrinsic Localized Modes in Anharmonic Crystals. Phys. Rev. Lett. 1988;61(8):970–973. DOI: 10.1103/PhysRevLett.61.970.
11. Dmitriev SV, Korznikova EA, Baimova YA, Velarde MG. Discrete breathers in crystals. Phys. Usp. 2016;59(5):446–461. DOI: 10.3367/UFNe.2016.02.037729.
12. Dorignac J, Zhou J, Cambell DK. Discrete breathers in nonlinear Schrodinger hypercubic lattices with arbitrary power nonlinearity. Physica D. 2008;237(4):486–504. DOI: 10.1016/j.physd.2007.09.018.
13. Gómez-Gardeñes J, Floría LM, Bishop AR. Discrete breathers in two-dimensional anisotropic nonlinear Schrodinger lattices. Physica D. 2006;216(1):31–43. DOI: 10.1016/j.physd.2005.12.017.
14. Babicheva RI, Semenov AS, Soboleva EG, Kudreyko AA, Zhou K, Dmitriev SV. Discrete breathers in a triangular beta-Fermi-Pasta-Ulam-Tsingou lattice. Phys. Rev. E. 2021;103(5):052202. DOI: 10.1103/PhysRevE.103.052202.
15. Korznikova EA, Morkina AY, Singh M, Krivtsov AM, Kuzkin VA, Gani VA, Bebikhov YV, Dmitriev SV. Effect of discrete breathers on macroscopic properties of the Fermi-Pasta-Ulam chain. Eur. Phys. J. B. 2020;93(7):123. DOI: 10.1140/epjb/e2020-10173-7.
16. Kolesnikov ID, Shcherbinin SA, Bebikhov YV, Korznikova EA, Shepelev IA, Kudreyko AA, Dmitriev SV. Chaotic discrete breathers in bcc lattice. Chaos, Solitons and Fractals. 2024;178: 114339. DOI: 10.1016/j.chaos.2023.114339.
17. Bachurina OV. Linear discrete breather in fcc metals. Computational Materials Science. 2019;160: 217–221. DOI: 10.1016/j.commatsci.2019.01.014.
18. Bachurina OV. Plane and plane-radial discrete breathers in fcc metals. Modelling Simul.

Mater. Sci. Eng. 2019;27(5):055001. DOI: 10.1088/1361-651X/ab17b7.
19. Bachurina OV, Kudreyko AA. Two-dimensional discrete breathers in fcc metals. Computational Materials Science. 2020;182:109737. DOI: 10.1016/j.commatsci.2020.109737.
20. Bachurina OV, Kudreyko AA. Two-component localized vibrational modes in fcc metals. Eur. Phys. J. B. 2021;94(11):218. DOI: 10.1140/epjb/s10051-021-00227-3.
21. Haas M, Hizhnyakov V, Shelkan A, Klopov M, Sievers AJ. Prediction of high-frequency intrinsic localized modes in Ni and Nb. Physical Review B. 2011;84(14):144303. DOI: 10.1103/PhysRevB.84.144303.
22. Krylova KA, Lobzenko IP, Semenov AS, Kudreyko AA, Dmitriev SV. Spherically localized discrete breathers in bcc metals V and Nb. Comp. Mater. Sci. 2020;180:109695. DOI: 10.1016/j.commatsci.2020.109695.
23. Murzaev RT, Kistanov AA, Dubinko VI, Terentyev DA, Dmitriev SV. Moving discrete breathers in bcc metals V, Fe and W. Comp. Mater. Sci. 2015;98:88–92. DOI: 10.1016/j.commatsci.2014.10.061.
24. Bachurina OV, Murzaev RT, Kudreyko AA, Dmitriev SV, Bachurin DV. Atomistic study of two-dimensional discrete breathers in hcp titanium. Eur. Phys. J. B. 2022;95(7):104. DOI: 10.1140/epjb/ s10051-022-00367-0.
25. Bachurina OV, Murzaev RT, Semenov AS, Korznikova EA, Dmitriev SV. Properties of moving discrete breathers in beryllium. Phys. Solid State. 2018;60(5):989–994. DOI: 10.1134/S1063783418050049.
26. Murzaev RT, Bachurin DV, Korznikova EA, Dmitriev SV. Localized vibrational modes in diamond. Phys. Lett. A. 2017;381(11):1003–1008. DOI: 10.1016/j.physleta.2017.01.014.
27. Voulgarakis NK, Hadjisavvas G, Kelires PC, Tsironis GP. Computational investigation of intrinsic localization in crystalline Si. Physical Review B. 2004;69(11):113201. DOI: 10.1103/PhysRevB.69.113201.
28. Zakharov PV, Starostenkov MD, Dmitriev SV, Medvedev NN, Eremin AM. Simulation of the interaction between discrete breathers of various types in a Pt_3Al crystal nanofiber. J. Exp. Theor. Phys. 2015;121(2):217–221. DOI: 10.1134/S1063776115080154.
29. Zakharov PV, Korznikova EA, Dmitriev SV, Ekomasov EG, Zhou K. Surface discrete breathers in Pt3Al intermetallic alloy. Surface Science. 2019;679:1–5. DOI: 10.1016/j.susc.2018.08.011.
30. Sakhnenko VP, Chechin GM. Symmetry selection rules in nonlinear dynamics of atomic systems. Doklady Physics. 1993;38:219–220.
31. Sakhnenko VP, Chechin GM. Bushes of modes and normal vibrations in nonlinear dynamical systems with discrete symmetry. Dokl. Math. 1994;39(9):625–628.
32. Chechin GM, Sakhnenko VP. Interactions between normal modes in nonlinear dynamical systems with discrete symmetry. Exact results. Physica D. 1998;117(1–4):43–76. DOI: 10.1016/S0167-2789(98)80012-2.
33. Daumont I, Dauxois T, Peyrard M. Modulational instability: First step towards energy localization in nonlinear lattices. Nonlinearity. 1997;10(3):617–630. DOI: 10.1088/0951-7715/10/3/003.
34. Doi Y, Nakatani A, Yoshimura K. Modulational instability of zone boundary mode and band edge modes in nonlinear diatomic lattices. Phys. Rev. E. 2009;79(2):026603. DOI: 10.1103/PhysRevE.79.026603.
35. Zhang XC, Shkurinov A, Zhang Y. Extreme terahertz science. Nature Photon. 2017;11(1):16–18. DOI: 10.1038/nphoton.2016.249.
36. Hafez HA, Chai X, Ibrahim A, Mondal S, Férachou D, Ropagnol X, Ozaki T. Intense terahertz radiation and their applications. J. Opt. 2016;18(9):093004. DOI: 10.1088/2040-8978/18/9/093004.

37. Chechin GM, Ryabov DS, Zhukov KG. Stability of low-dimensional bushes of vibrational modes in the Fermi-Pasta-Ulam chains. Physica D. 2005;203(3–4):121–166. DOI: 10.1016/ j.physd.2005.03.009.
38. Chechin GM, Sizintsev DA, Usoltsev OA. Nonlinear atomic vibrations and structural phase transitions in strained carbon chains. Comp. Mater. Sci. 2017;138:353–367. DOI: 10.1016/ j.commatsci.2017.07.004.
39. Morkina AY, Singh M, Bebikhov YV, Korznikova EA, Dmitriev SV. Variation of the Specific Heat in the Fermi–Pasta–Ulam Chain due to Energy Localization. Phys. Solid State. 2023;64:446–454. DOI: 10.1134/S1063783422090050.
40. Abdullina DU, Semenova MN, Semenov AS, Korznikova EA, Dmitriev SV. Stability of delocalized nonlinear vibrational modes in graphene lattice. Eur. Phys. J. B. 2019;92(11):249. DOI: 10.1140/ epjb/e2019-100436-y.
41. Upadhyaya A, Semenova MN, Kudreyko AA, Dmitriev SV. Chaotic discrete breathers and their effect on macroscopic properties of triangular lattice. Communications in Nonlinear Science and Numerical Simulation. 2022;112:106541. DOI: 10.1016/j.cnsns.2022.106541.
42. Shcherbinin SA, Krylova KA, Chechin GM, Soboleva EG, Dmitriev SV. Delocalized nonlinear vibrational modes in fcc metals. Communications in Nonlinear Science and Numerical Simulation. 2022;104:106039. DOI: 10.1016/j.cnsns.2021.106039.
43. Babicheva RI, Semenov AS, Shcherbinin SA, Korznikova EA, Kudreyko AA, Vivegananthan P, Zhou K, Dmitriev SV. Effect of the stiffness of interparticle bonds on properties of delocalized nonlinear vibrational modes in an fcc lattice. Phys. Rev. E. 2022;105(6):064204. DOI: 10.1103/ PhysRevE.105.064204.
44. Morkina AY, Bachurin DV, Dmitriev SV, Semenov AS, Korznikova EA. Modulational instability of delocalized modes in fcc copper. Materials. 2022;15(16):5597. DOI: 10.3390/ ma15165597.
45. Bachurina OV, Murzaev RT, Shcherbinin SA, Kudreyko AA, Dmitriev SV, Bachurin DV. Multi-component delocalized nonlinear vibrational modes in nickel. Modelling Simul. Mater. Sci. Eng. 2023;31:075009. DOI: 10.1088/1361-651X/acf14a.
46. Bachurina OV, Murzaev RT, Shcherbinin SA, Kudreyko AA, Dmitriev SV, Bachurin DV. Delocalized nonlinear vibrational modes in Ni_3Al. Communications in Nonlinear Science and Numerical Simulation. 2024;132:107890. DOI: 10.1016/j.cnsns.2024.107890.
47. Ostropiko ES, Konstantinov AY. Stress-induced martensite formation under high strain rate loading in TiNi shape memory alloy. Lett. Mater. 2024;14(2):143–149. DOI: 10.48612/ letters/2024-2-143-149.
48. Rubanik VV, Bahrets DA, Rubanik VV, Urban VI, Dorodeiko VG, Andreev VA, Chekan NM, Akula IP Effect Mechanical properties of TiNi medical alloy with bioinert coatings. Lett. Mater. 2023;13(4):353–356. DOI: 10.22226/2410-3535-2023-4-353-356.
49. Resnina NN, Ivanov AM, Belyaev FS, Volkov AE, Belyaev SP Simulation of recoverable strain variation during isothermal holding of the Ni51Ti49 alloy under various regimes. Lett. Mater. 2023;13(1):33–38. DOI: 10.22226/2410-3535-2023-1-33-38.
50. Bachurina OV, Kudreyko AA, Dmitriev SV, Bachurin DV. Impact of delocalized nonlinear vibrational modes on the properties of NiTi. Phys. Lett. A. 2025;555:130769. DOI: 10.1016/ j.physleta.2025.130769.
51. Thompson AP, Aktulga HM, Berger R, Bolintineanu DS, Brown WM, Crozier PS, Veld PJI, Kohlmeyer A, Moore SG, Nguyen TD, Shan R, Stevens MJ, Tranchida J, Trott C, Plimpton SJ. LAMMPS-a flexible simulation tool for particle-based materials modeling at the atomic, meso, and continuum scales. Computer Physics Communications. 2022;271:108171. DOI: 10.1016/j.cpc.2021.108171.
52. LAMMPS [Electronic resource]. Available from: http://lammps.sandia.gov.

53. Kim YK, Kim HK, Jung WS, Lee BJ. Development and application of Ni-Ti and Ni-Al-Ti 2NN-MEAM interatomic potentials for Ni-base superalloys. Comp. Mater. Sci. 2017;139: 225–233. DOI: 10.1016/j.commatsci.2017.08.002.
54. Singh M, Morkina AY, Korznikova EA, Dubinko VI, Terentiev DA, Xiong DX, Naimark OB, Gani VA, Dmitriev SV. Effect of discrete breathers on the specific heat of a nonlinear chain. J. Nonlinear Sci. 2021;31(1):12. DOI: 10.1007/s00332-020-09663-4.
55. Naumov EK, Bebikhov YV, Ekomasov EG, Soboleva EG, Dmitriev SV. Discrete breathers in square lattices from delocalized nonlinear vibrational modes. Phys. Rev E. 2023;107(3): 034214. DOI: 10.1103/PhysRevE.107.034214.
56. Bachurin DV, Murzaev RT, Abdullina DU, Semenova MN, Bebikhov YV, Dmitriev SV. Chaotic discrete breathers in bcc lattice: Effect of the first- and second interactions. Physica D. 2024;470: 134344. DOI: 10.1016/j.physd.2024.134344.
57. Bebikhov YV, Naumov EK, Semenova MN, Dmitriev SV. Discrete breathers in a β-FPUT square lattice from in-band external driving. Communications in Nonlinear Science and Numerical Simulation. 2024;132:107897. DOI: 10.1016/j.cnsns.2024.107897.
58. Shcherbinin SA, Bebikhov YV, Abdullina DU, Kudreyko AA, Dmitriev SV. Delocalized nonlinear vibrational modes and discrete breathers in a body centered cubic lattice. Communications in Nonlinear Science and Numerical Simulation. 2024;135:108033. DOI: 10.1016/j.cnsns.2024.108033.
59. Shepelev IA, Soboleva EG, Kudreyko AA, Dmitriev SV. Influence of the relative stiffness of second-neighbor interactions on chaotic discrete breathers in a square lattice. Chaos, Solitons and Fractals. 2024;183:114885. DOI: 10.1016/j.chaos.2024.114885.
60. Shcherbinin SA, Kazakov AM, Bebikhov YV, Kudreyko AA, Dmitriev SV. Delocalized nonlinear vibrational modes and discrete breathers in β-FPUT simple cubic lattice. Phys. Rev. E. 2024;109(1): 014215. DOI: 10.1103/PhysRevE.109.014215.